



1 Equifinality Contaminates the Sensitivity Analysis of Process- 2 Based Snow Models

3 Tek Kshetri¹, Amir Khatibi², Yiwen Mok³, M Shahabul Alam⁴, Hongli Liu⁵, Martyn P. Clark⁶

4

5 ¹Water, Sediment, Hazards, & Earth-surface Dynamics (waterSHED) Lab, University of Calgary, Canada

6 ²Department of Civil, Geological and Environmental Engineering, University of Saskatchewan, Canada

7 ³Department of Civil Engineering, Faculty of Engineering, Universiti Putra Malaysia (UPM), Serdang, Malaysia

8 ⁴Alabama Water Institute, The University of Alabama, USA

9 ⁵Department of Civil and Environmental Engineering, University of Alberta, Canada

10 ⁶Department of Civil Engineering, University of Calgary, Canada

11

12 *Correspondence to:* Amir Khatibi (amir.khatibi@usask.ca), Tek Kshetri (iamtekson@email.com)

13

14 Abstract

15 This study assesses the impact of different flux parameterizations and model parameters on simulations of snow depth.
16 Through a sensitivity analysis in a process-based snow model based on the SUMMA framework, various options for
17 parametrizing snow processes and adjusting parameter values were evaluated to identify optimal modeling
18 approaches, understand sources of uncertainty, and determine reasons for model weaknesses. The study focused on
19 model parameterizations of precipitation partitioning, liquid water flow, snow albedo, atmospheric stability, and
20 thermal conductivity. In this study, sensitivity analysis (SA) is performed using the one-at-a-time (OAT) SA method
21 as well as the Morris Method to estimate Elementary Effects, aiming to further explore the magnitudes and patterns
22 of sensitivities. The sensitivity analyses in this study are used to evaluate process parameterizations, model parameter
23 values, and model configurations. Performance metrics such as the Nash-Sutcliffe Efficiency (NSE), the Kling-Gupta
24 Efficiency (KGE), the root mean squared log error (RMSLE), and mean are used to assess the similarity between
25 simulated and observed data. Bootstrapping is employed to estimate the variability of mean Elementary Effects and
26 establish confidence bounds. The key findings of this research indicate that sensitivity analysis of snow modelling
27 parameters plays a crucial role in understanding their impact on decision outcomes. The study identified the most
28 sensitive parameters, such as critical temperature and thermal conductivity of snow, as well as liquid water drainage
29 parameters. It was observed that water balance fluxes exhibited higher sensitivity than energy balance fluxes in
30 simulating snow processes. The analysis also highlighted the importance of accurately representing water balance
31 processes in snow models for improved accuracy and reliability. A key finding in this study is that the sensitivity of
32 performance metrics to model parameters is contaminated by equifinality (i.e., parameter perturbations lead to similar
33 performance metrics for quite different snow depth time series), and hence many published parameter sensitivity
34 studies may provide misleading results. These findings have implications for snow hydrology research and water
35 resource management, providing valuable insights for optimizing snow modelling and enhancing decision-making.

36

37 **Keywords:** Snow Modelling, Sensitivity Analysis, Morris Method, Performance Metrics, Equifinality, SUMMA

38

39 1 Introduction

40

41 Hydrological models differ in their conceptualization and implementation to the extent that there is typically little
42 agreement regarding "correct" model structures, particularly at larger spatial scales (Clark et al., 2011; Gupta et al.,



43 2012). Hydrological modelling decisions are often made in an ad-hoc manner, depending on the purpose of the
44 modelling study, the understanding of hydrological processes, the availability of data for the model evaluation, and
45 other considerations (Clark et al., 2011). The wide range of decisions made by various modelers to account for the
46 complex and interdisciplinary challenge of developing process-based hydrological models has led to the proliferation
47 of hydrological models (Clark et al., 2011; 2015b), making it difficult to clearly attribute model performance
48 differences to specific decisions that are made as part of the model development process (Koster and Milly, 1997). As
49 a result, a key challenge for the hydrological modelling community has been to evaluate the underlying hypotheses of
50 hydrological models, and to further improve models for specific applications (Clark et al., 2011).

51

52 The objective of this study is to conduct a sensitivity analysis to evaluate the impact of alternative flux
53 parameterizations and different model parameters on snow depth in a process-based snow model. To this end, this
54 study uses the SUMMA framework (described in the next section) to conduct a sensitivity analysis on snow modelling
55 processes in the Reynolds Mountain East research catchment. An Elementary Effects method is used to evaluate the
56 options used to parametrize snow modelling processes and the parameter values that are used in the model
57 parameterizations. This work is useful to identify preferable modelling approaches, understand various sources of
58 model uncertainty, and determine specific reasons for model weaknesses. The snow process parameterizations we
59 consider include precipitation partitioning, liquid water flow, snow albedo, atmospheric stability, and thermal
60 conductivity.

61 The remainder of this paper is organized as follows. Section 2 describes the methods used to conduct sensitivity
62 analysis of process-based snow models. Section 3 presents the results and discussion, and Section 4 provides some
63 key conclusions from this study.

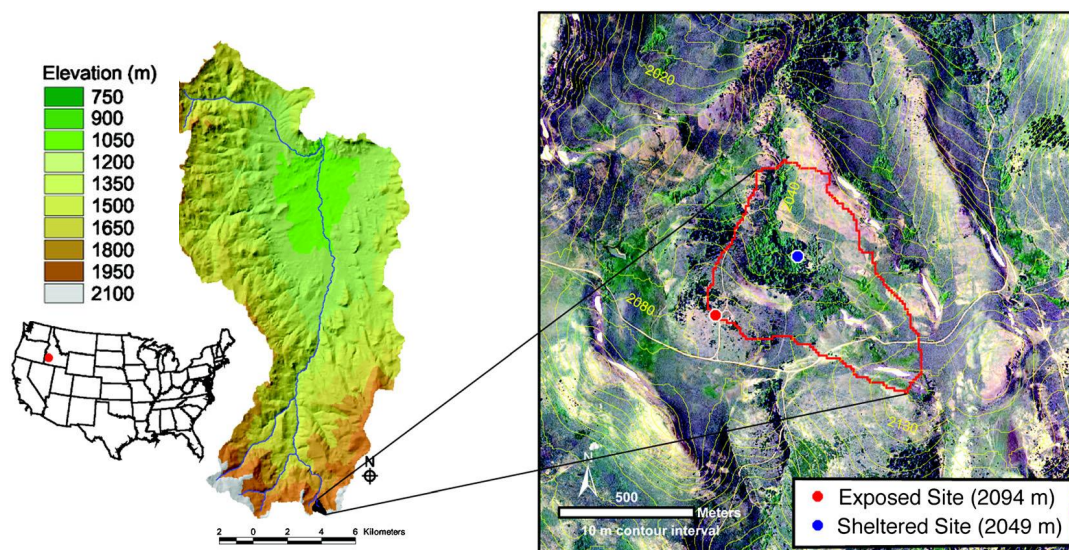
64 **2 Methodology**

65 **2.1 Study Area**

66 Reynolds Mountain East is located in southwestern Idaho (Flerchinger et al., 2012; Reba et al., 2009, 2014, 2011,
67 2012). It is a headwater catchment in southwestern Idaho's Reynolds Creek Experimental Watershed (RCEW) (Robins
68 et al., 1965). RCEW's geography varies from a flat valley in the north to steep mountain slopes in the south, with an
69 elevation range of 1099 to 2244 m above mean sea level and an area of 239 km² (Sridhar and Nayak, 2010). The
70 elevation over RCEW causes orographic effects, which cause a decrease in temperature and a rise in precipitation.
71 The lower elevations of RCEW receive 4-5 times less precipitation than those at higher elevations (Hanson et al.,
72 2001). At higher elevations, snow predominates, while rain takes over at lower elevations and in the watershed's valley
73 regions. The Reynolds Mountain East (RME) watershed receives approximately 900 mm of precipitation each year,
74 with over 70% of it falling as snow, and about 520 mm of this precipitation exits the basin as stream flow (Seyfried et
75 al., 2009). Snow tends to accumulate in deep drifts, often exceeding 2 meters in sheltered areas (Winstral and Marks,
76 2014).

77

78 The data from the “sheltered site” (i.e., the Aspen site) in Reynolds Mountain East (RME) was used to investigate
79 how simulations of snow depth are affected by the process parameterizations and parameter values, including the
80 thermal conductivity of snow, snow albedo, and the critical temperature that is used to distinguish rain from snow.
81 The sheltered site is located in a clearing in a forest, where the grasses are covered by snow early in the snow season
82 and vegetation has little influence on how the snow depth changes during the year (Figure 1). In addition, protected
83 locations have modest wind speeds (Reba et al., 2011), thus turbulent heat fluxes have less impact on the surface
84 energy balance than in more exposed locations. The annual development of the snowpack is mostly governed by the
85 surface radiation budget. The available observed snow depth data spans from October 1999 to October 2008.



86

87 **Figure 1:** Location map of Reynolds Mountain East Catchment (Reba et al. 2012, 2014)

88

89 This study simulates snow processes for the period November 2005 to June 2006. This choice was made to reduce the
90 computational effort required for modelling and analysis. Additionally, the time interval between November and June
91 was specifically chosen as it reflects a complete cycle of snow accumulation and melting, with non-zero snow depth
92 values throughout this period. However, selecting the 2005-2006 year does not offer any advantage over choosing
93 other years since the snow depth pattern remains almost consistent throughout the recorded period.

94 2.2 The SUMMA multiple hypothesis framework

95 A model can be considered as an assemblage of coupled hypotheses that describe dominant hydrological processes
96 (Clark et al., 2011). In this respect, it is important to investigate hypotheses that define individual processes and their
97 connections within the overall system (Clark et al., 2011); i.e., to adopt the "multiple working hypotheses" approach
98 defined by Chamberlin (1890) to investigate multiple rational explanations for the phenomenon being studied. This
99 approach also provides a systematic approach to model evaluation and improvement (Clark et al., 2011). Some
100 examples of multiple hypothesis frameworks are JULES (Best et al., 2011), CLM (Lawrence and Chase, 2007), Noah-
101 MP (Niu et al., 2011), and SUMMA (Clark et al. 2015b).

102 This study uses the Structure for Unifying Multiple Modeling Alternatives (SUMMA), a flexible, extensible, and
103 modular framework to simulate hydrological processes. SUMMA's modular structure enables incorporating different
104 model representations of physical processes in a common set of conservation equations, which makes it possible to
105 systematically evaluate different parameterizations of the same process and understand the impact of different
106 modelling assumptions on model behavior (Clark et al. 2015b). SUMMA is an example of a multiple hypothesis
107 framework (Clark et al., 2011), which enables users to identify process parameterizations consistent with theoretical
108 expectations and observed data, and to characterize model uncertainty through much more extensive and detailed
109 coverage of the model hypothesis space than typical small ensemble multimodel applications.



110 **2.3 Snow Modelling Parametrizations and Parameters in SUMMA**

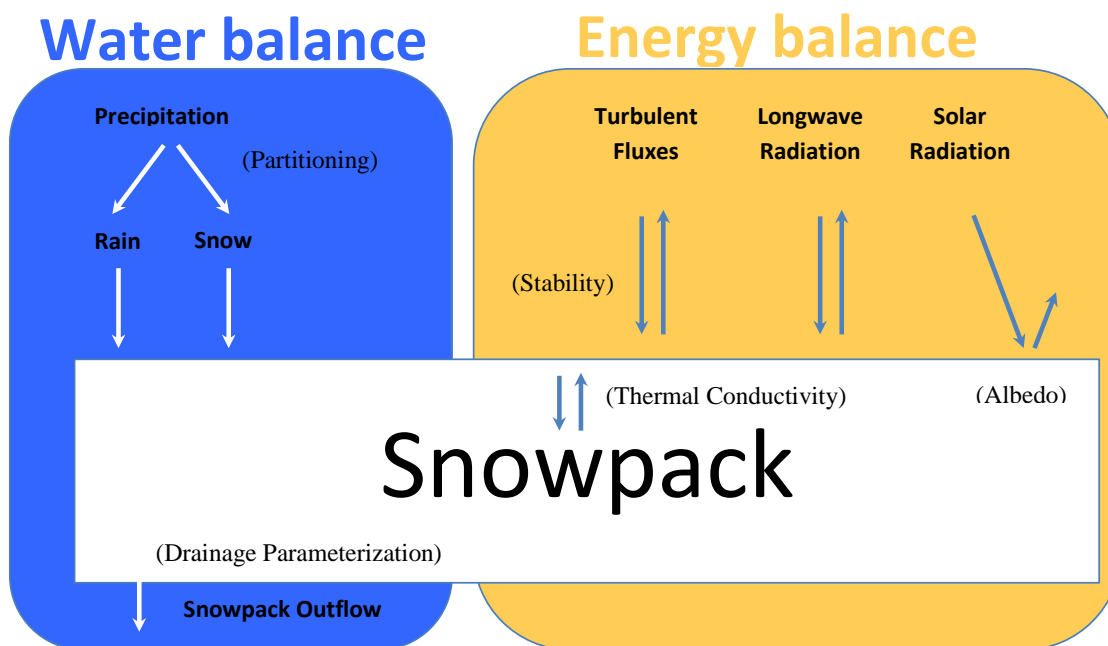
111 SUMMA includes five key processes for snow modelling; 1. Precipitation partitioning; 2. Liquid water flux through
112 snowpack; 3. Snow albedo; 4. Atmospheric stability; and 5. Thermal conductivity. The precipitation partitioning and
113 liquid water in snowpack flux are used in the water balance equations, whereas albedo, atmospheric stability, and
114 thermal conductivity are used in the energy balance equations. The summary of the parameters are listed in Table 1.

115

116 Figure 2 summarizes the water and energy balance fluxes that are calculated in SUMMA. This study employs various
117 parametrizations of these fluxes for the snowpack simulation, which are detailed below.

118

119



120 **Figure 2:** The water and energy balance fluxes used in the SUMMA snow modelling simulations.

121

122 Each hydrologic process can be expressed by one or more different parameterizations (i.e., equations or formulas).

123 Each parameterization includes different numbers of parameters. Table 1 summarizes all the parameters together with

124 their associated range used for snow modeling, on which sensitivity analysis will be conducted. The detailed

125 explanation of each parameterization is explained in Appendix A.

126

127

128

129



130 **Table 1:** Summary and range of parameters used for sensitivity analysis

Flux	Parameterizations	Parameters (Unit)	Default value	Min.	Max.
Precipitation flux	Function of wet-bulb temperature (Marks et al., 2013)	Critical temperature (K)	273.16	272.16	274.16
Liquid water in snowpack flux	Gravity drainage (Colbeck, 1976; Colbeck and Anderson, 1982)	Capillary retention (K)	0.06	0.01	0.1
		Hydraulic conductivity of snow (m s^{-1})	0.015	0.005	0.05
		Exponent for meltwater flow (-)	3.0	1.0	5.0
Atmospheric stability	Standard (Anderson, 1976)	Critical Richardson Number (-)	0.2	0.1	1.0
	Louisinv (Louis, 1979)	Louis79 “b” parameter (-)	9.4	9.2	9.6
	MahrtExp (Mahrt, 1987)	Mahrt87 eScale (-)	1.0	0.5	2.0
Thermal conductivity	smnv 2000 (Smirnova et al., 2000)	Fixed thermal conductivity ($\text{W K}^{-1} \text{m}^{-1}$)	0.35	0.10	1.00
Albedo	Constant decay (Verseghy, 1991)	Constant albedo decay rate (-)	1.0d+6	1.0d+5	5.0d+6
	Variable decay (Yang et al., 1997)	Variable albedo decay rate (-)	1.0d+6	1.0d+5	5.0d+6
		Temperature scale growth (-)	0.04	0.02	0.06
		Albedo soot load (-)	0.3	0.1	0.5

131

132

133 **2.4 Sensitivity Analysis**

134 Sensitivity analysis is used to evaluate how the model responds to differences in “input factors” in the model
 135 instantiation. The input factors can be the meteorological forcing data, the model parameters, or the subjective
 136 decisions that are made as part of model development (e.g., the choice of process parameterizations). The model
 137 response to differences in input factors are typically characterized using summary statistics of model behavior (e.g.,
 138 an average model flux) or summary statistics of model performance (e.g., the sum of squared differences between
 139 model simulations and observations).



140 In this study, sensitivity analysis is performed in SUMMA using local or one-at-a-time (OAT) methods as well as the
141 Morris Method to estimate Elementary Effects to assess the selection of parameterizations (i.e., equations used to
142 parameterize specific processes), the selection of model parameters used in the parameterizations (i.e., the model
143 equations), and the model discretization configurations (Clark et al. 2015b). The sensitivity analysis was completed
144 using the online collaboration environment operated by the Consortium of Universities for the Advancement of
145 Hydrologic Science, Incorporated (CUAHSI). CUAHSI provides a cloud computing service called CUAHSI
146 Community JupyterHub (Tarboton et al., 2024), which includes pre-installed Python wrappers around the SUMMA
147 model (pySumma).

148 The following sections provide details of the summary statistics examined as well as the Elementary Effects (EE)
149 method that is used for sensitivity analysis.

150 2.4.1 The Elementary Effects method (Morris method)

151 The Elementary Effects (EE) method is a simple yet efficient approach to sifting through numerous input factors in a
152 model and identifying the significant ones. Morris conceived the concept of elementary effects in 1991, suggesting
153 the creation of two sensitivity measures to gauge the impact of input factors as negligible, linear and additive, or
154 nonlinear and intertwined with other factors (Saltelli et al., 2008).

155 Based on the one-at-a-time method, an individual trajectory is created by perturbing each parameter p_i by a variation
156 Δ_i . The number of perturbations of each trajectory is equal to the number of input factors ($i = 1, 2, \dots, k$). The EE of the
157 i^{th} parameter (EE_i) is calculated as follows:

$$158 \quad EE_i = \frac{f(X_{p_i+\Delta_i}) - f(X|_{p_i})}{\Delta_i}$$

159 where $f(X)$ denotes the performance metrics used for sensitivity analysis. Here we used four metrics as will be
160 discussed in the next section. Starting from multiple points within the feasible parameter space, multiple trajectories
161 (r) are generated to compute the sensitivity indices, i.e., the mean of EEs (μ_i^*) denoting the global sensitivity of each
162 parameter and the standard deviation of EEs (σ_i) denoting the interaction with other parameters. The equation below
163 gives the calculations of these indices suggested by Campolongo et al. (2007):

$$164 \quad \mu_i^* = \frac{1}{r} \sum_{j=1}^r |EE_i^j|, \sigma_i = \sqrt{\frac{1}{r-1} \sum_{j=1}^r (EE_i^j - \mu_i^*)^2},$$

165 where EE_i^j denotes the EE_i of the j^{th} trajectory.

166 In summary, to compute each elementary effect, r trajectories of $(k+1)$ points in the input space are required, where k
167 represents the number of input factors. Each trajectory provides k elementary effects, one per input factor, resulting in
168 $r(k+1)$ sample points in total. An $r = 20$ which is twice more than the typical number of trajectories was selected to
169 generate the sampling data for each of the parametrizations.

170 Matrices of sampling data were produced using SAFEpython (Pianosi et al., 2015; Noacco et al., 2019) where the
171 results were further validated against the principles of the Morris method to ensure the generation of accurate values.
172 The performance metrics used for the sensitivity analysis are discussed in the next section.

173 2.4.2 Performance metrics

174 The similarity between the simulated and observed snow depth values over the runtime period was expressed in a
175 single number using a set of performance/evaluation metrics: The performance metrics used in this study are the Nash-



176 Sutcliffe Efficiency (NSE; Nash and Sutcliffe, 1970), the Kling-Gupta Efficiency (2012) (KGE; Gupta et al., 2009;
 177 Kling et al., 2012), the root mean squared log error (RMSLE; Willmott and Matsuura, 2005) and the Mean. These
 178 four metrics provide different evaluation perspectives of flow simulation results, and each will identify in a distinct
 179 manner the extent to which altering a parameter influences the outcome of a decision. Accordingly, using these metrics
 180 together with qualitative sensitivity analysis methods will help identify model configurations that closely predict the
 181 overall system behavior.

182 Table 2 defines the four performance metrics, where n is the total number of events; O_i and S_i are the observed data
 183 and simulated data; \underline{O} is the corresponding mean values; σ_o and σ_s represent the standard deviation of the observed
 184 and simulated values; μ_o and μ_s represent the mathematical expectation of the observed and simulated values,
 185 respectively.

186 **Table 2:** Description of the performance metrics

Metrics	Equation	Scope
Nash-Sutcliffe Efficiency (NSE)	$NSE = 1 - \frac{\sum_{i=1}^n (S_i - O_i)^2}{\sum_{i=1}^n (O_i - \underline{O})^2}$	$-\infty < NSE < 1$
Kling-Gupta Efficiency 2012 (KGE)	$KGE_{2012} = 1 - ED$ $ED = \sqrt{(s[1] \cdot (r - 1))^2 + (s[2] \cdot (\gamma - 1))^2 + (s[3] \cdot (\beta - 1))^2}$ <p><i>s (tuple of length three) = Represents the scaling factors to be used for re-scaling of the coefficients.</i> <i>r = Pearson Correlation Coefficient</i></p> $\beta = \mu_s / \mu_o$ $\gamma = \frac{CV_s}{CV_o} = \frac{\sigma_s / \mu_s}{\sigma_o / \mu_o}$	$-\infty < KGE (2012) < 1$
Root Mean Squared Log Error (RMSLE)	$RMSLE = \left(\frac{1}{n} \sum_{i=0}^n \left(\ln \ln \left(\frac{S_i}{O_i} \right) \right)^2 \right)^{\frac{1}{2}}$	$0 \leq RMSLE \leq \infty$
Mean (average snow depth)	$Mean = \frac{1}{n} \sum_{i=0}^n (S_i)$	$0 \leq Mean < \infty$

187 The NSE is a commonly used metric that normalizes model performance into an interpretable scale (Knoben et al.,
 188 2019). One main drawback of the NSE is that it punishes a higher variance in the observed values (Roberts et al.,
 189 2018). Gupta et al. (2009) developed KGE (2009) in the context of hydrologic modelling to explain the relative
 190 significance of correlation, bias, and variability to address issues associated with the NSE. Further, Kling et al. (2012)
 191 proposed KGE (2012) as an enhanced version of KGE (2009) in order to prevent cross-correlation between variability
 192 ratios and bias. Larger values of NSE and KGE indicate a stronger agreement between observations and simulations.
 193 When the metric values for NSE, Mean, and RMSLE are all zero, or for KGE when the value is -0.41, it indicates that
 194 the model simulations have the same explanatory power as the mean of the observations (Knoben et al., 2019). The
 195 RMSLE limits the impact of outliers by more evenly weighting high and low values. Smaller values indicate a stronger
 196 correspondence between observations and simulations (Roberts et al., 2018).

197 Performance metrics were calculated utilizing the HydroErr Python package (Roberts et al., 2018). The metrics were
 198 computed for each simulation run, with the number of simulations for each parametrization being $r(k+1)$, as described



199 in section 3.3.1. This enabled the calculation of Elementary Effects for each parametrization. Bootstrapping was used
200 as a resampling technique to estimate the variability of mean Elementary Effects and to develop confidence bounds.
201 The method involved randomly selecting a sample from the original data set and generating multiple resampled data
202 sets of the same size as the original data set. Then, the mean Elementary Effects were calculated for each resampled
203 data set, resulting in a distribution of the means. Confidence bounds were then determined by calculating the 25th,
204 50th, and 75th percentiles.

205 **3 Results and Discussion**

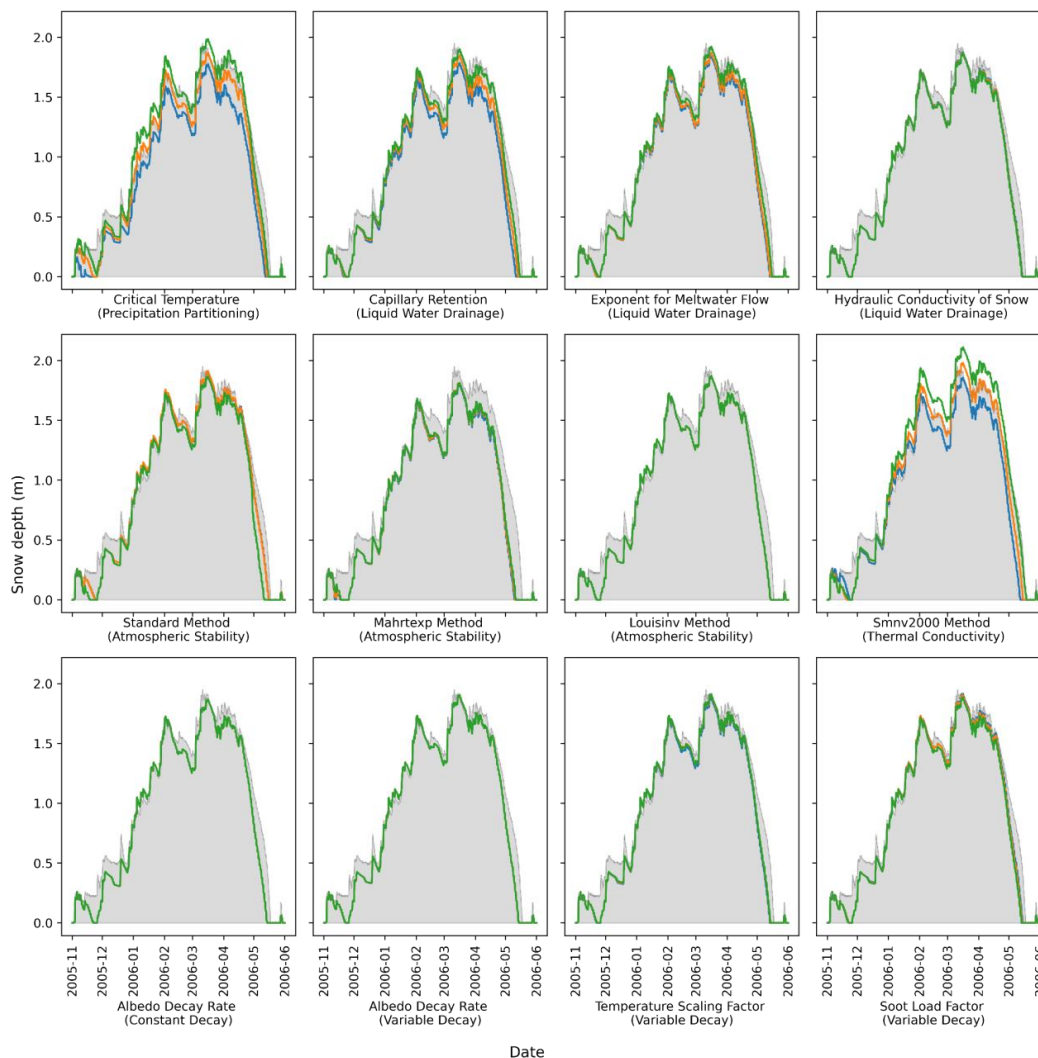
206

207 In this section, we outline our systematic approach to analyzing parameter sensitivities within our snow modeling
208 study. We begin by utilizing SUMMA to conduct simulations under varying parameter perturbations. These
209 preliminary simulations enable identifying potentially sensitive parameters, offering initial insights into their impact
210 on snow depth predictions. Subsequently, we quantitatively assess sensitivities using sensitivity indices derived from
211 diverse performance metrics (Mean, KGE, MSE, and RMSLE). This comprehensive analysis highlights the agreement
212 between simulations and observations across different parameterizations, revealing the potential influence of specific
213 parameters on specific performance metrics. Additionally, we employ the Morris Method to estimate Elementary
214 Effects, aiming to further explore the magnitudes and patterns of sensitivities. This method aids in characterizing
215 parameter impacts and contributes to a deeper understanding of the complex interplay between parameters and
216 simulation results. Overall, our approach enables a comprehensive examination of parameter sensitivities based on
217 specific performance metrics, providing specific parameters influence on the snow model.

218

219 **3.1 Snow depth perturbation**

220 SUMMA was used to run the parameters listed in Table 1 by altering one parameter at a time while maintaining a
221 default value for other parameters. Figure 4 illustrates the result of these simulations for 12 parameters and
222 parametrizations used for snow modelling in the Reynolds Mountain East research catchment. These snow depth
223 perturbation graphs are helpful to gain an initial understanding of potentially high and low sensitivity parameters.
224 Based on these initial sensitivity experiments, it is expected that the most sensitive parameter would be the critical
225 temperature and thermal conductivity of snow (Smnv2000 method), followed by the liquid water drainage parameters
226 (capillary retention and exponent of meltwater flow), and the critical Richardson Number (Standard atmospheric
227 stability method), respectively. Furthermore, it can be observed that snow depth calculation is relatively insensitive to
228 changes in snow albedo, as well as to the atmospheric stability methods of MahrtExp and Louisinv.



229
230

Figure 3: Snow depth perturbation plots for all parameters and available parameterization used in snow modelling processes (November 2005 to June 2006). The gray areas represent observed snow depth values, while the blue, orange, and green lines represent simulated snow depth values for the minimum, default, and maximum values of a parameter, respectively.

231
232
233
234
235
236
237

3.2 Confidence intervals and marginal errors

238
239
240
241
242

To quantify the magnitude and rank of sensitivity associated with each parameter, a more comprehensive One-at-A-Time sensitivity analysis is conducted to generate sensitivity indices for every parameter. Table 4 summarizes the mean of the 95% confidence interval \pm marginal error of the performance metrics. This helps to determine the result's precision and reliability and to assess the statistical significance of the results. The margin of error for four



243 performance metrics is relatively small, indicating a more precise estimate.

244

245 The reported values of Mean snow depth, NSE, KGE (2012), and RMSLE performance metrics provide a measure of
 246 how well the simulations using each parameterization capture the observed snow depth values. Overall, the
 247 performance results show a high degree of consistency between the simulated and observed snow depth data based on
 248 mean metric, regardless of the parameterizations. However, ranking of each parameter's sensitivity from least to most
 249 accurate slightly differs depending on the performance metric used. In general, the results suggest that the Louisinv
 250 parameterization/method is capable of providing more accurate predictions for estimating atmospheric stability as
 251 compared to the MahrtEXP and Standard methods, which show lower Mean, NSE, and KGE scores and a higher
 252 RMSLE score. The relatively higher accuracy of Louisinv is likely due to the iterative nature of the Louisinv method,
 253 which allows for a more precise calculation of the bulk Richardson number and eddy diffusivities for heat and
 254 moisture. It can also be observed that the accuracy of predictions is almost identical for constant and variable albedo
 255 decay rates. This suggests that the temporal changes in snow properties used for albedo calculation can be adequately
 256 captured through the accumulation and melting period decay curves at Reynolds Mountain East. Overall, the
 257 MahrtExp method is associated with the least accurate prediction, while the thermal conductivity and variable albedo
 258 decay parameterization are associated with the highest prediction accuracy.

259

260 **Table 4:** Performance metrics associated with each parameterization

Flux	Parameterization	Mean	KGE (2012)	NSE	RMSLE
Precipitation flux	Function of wet-bulb temperature (Marks et al., 2013)	0.933 ± 0.017	0.830 ± 0.017	0.939 ± 0.008	0.097 ± 0.005
Liquid water in snowpack flux	Gravity drainage (Colbeck, 1976; Colbeck and Anderson, 1982)	0.916 ± 0.008	0.819 ± 0.008	0.933 ± 0.008	0.101 ± 0.005
Atmospheric stability	Standard (Anderson, 1976)	0.931 ± 0.005	0.819 ± 0.010	0.940 ± 0.006	0.102 ± 0.005
	Louisinv (Louis, 1979)	0.924 ± 0.000	0.826 ± 0.000	0.944 ± 0.000	0.098 ± 0.000
	MahrtExp (Mahrt, 1987)	0.861 ± 0.002	0.747 ± 0.003	0.880 ± 0.002	0.137 ± 0.001
Thermal conductivity	smnv 2000 (Smirnova et al., 2000)	1.023 ± 0.015	0.850 ± 0.004	0.949 ± 0.003	0.085 ± 0.003
Albedo	Constant decay (Verseghy, 1991)	0.933 ± 0.002	0.834 ± 0.002	0.949 ± 0.001	0.094 ± 0.001
	Variable decay (Yang et al., 1997)	0.938 ± 0.002	0.835 ± 0.002	0.952 ± 0.001	0.093 ± 0.001

261

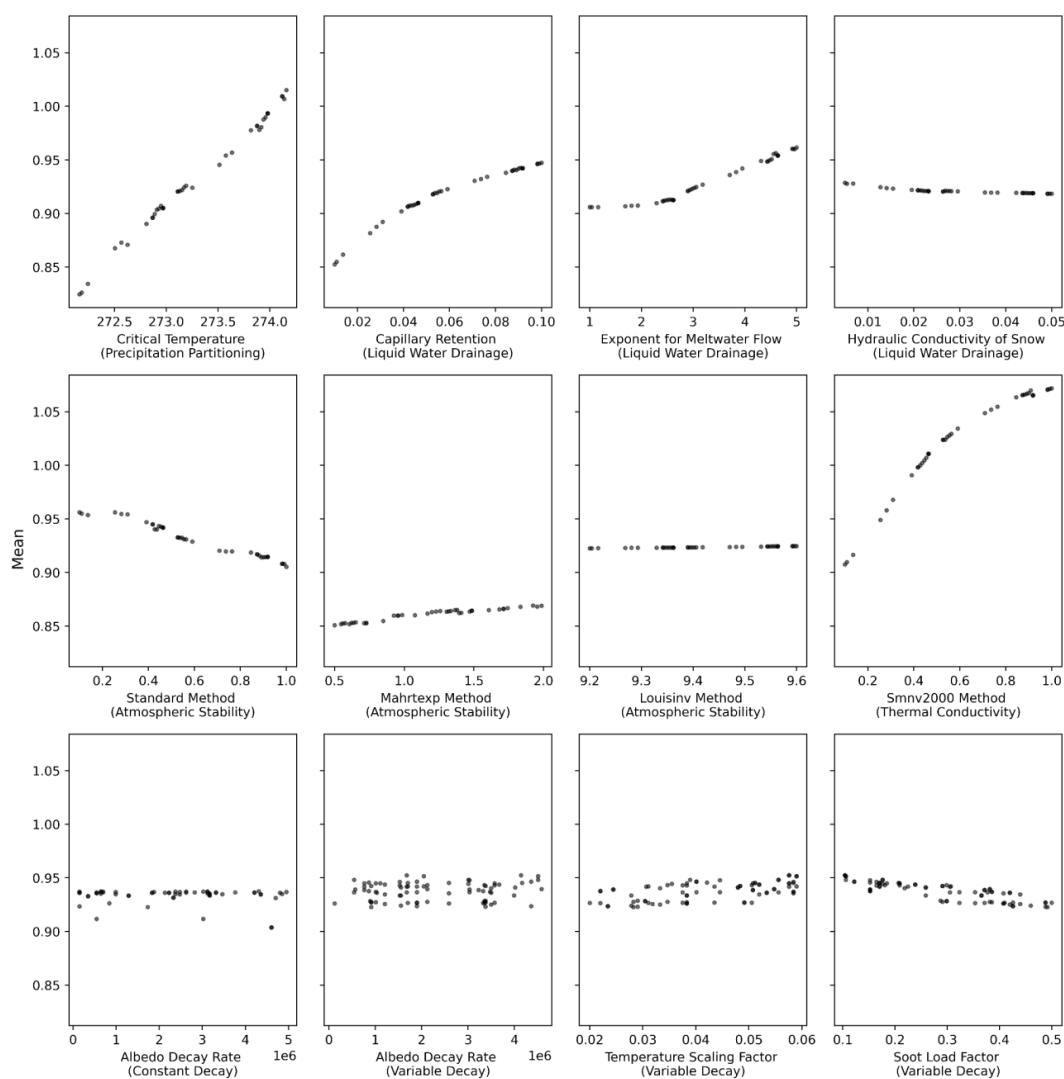
262

263 **3.3 Qualitative sensitivity analysis**

264 Figure 5 shows a scatter plot of all snow model parameters, where the mean snow depth is plotted against each
 265 parameter range. The purpose of this plot is to qualitatively visualize parameters with potentially high and low
 266 sensitivities, which can be useful for screening and ranking them. Parameters with higher variability are considered to



267 be more sensitive. Based on the observed patterns, it is expected that the constant and variable albedo parameters, as
 268 well as the hydraulic conductivity of the snowpack, will be the least sensitive. On the other hand, the critical
 269 temperature, thermal conductivity, capillary retention, and exponent for meltwater flow are likely to be the most
 270 sensitive parameters. Moreover, in cases where there is a discernible pattern in each parameter, it becomes possible to
 271 identify the optimum value that can lead to the highest level of agreement between the simulation and observation.
 272 For instance, the simulation of snow depth will improve for the values of the exponent for meltwater flow greater than
 273 2, but will not significantly improve for the thermal conductivity values greater than $0.8 [W K^{-1} m^{-1}]$.



274
 275
 276
 277
 278

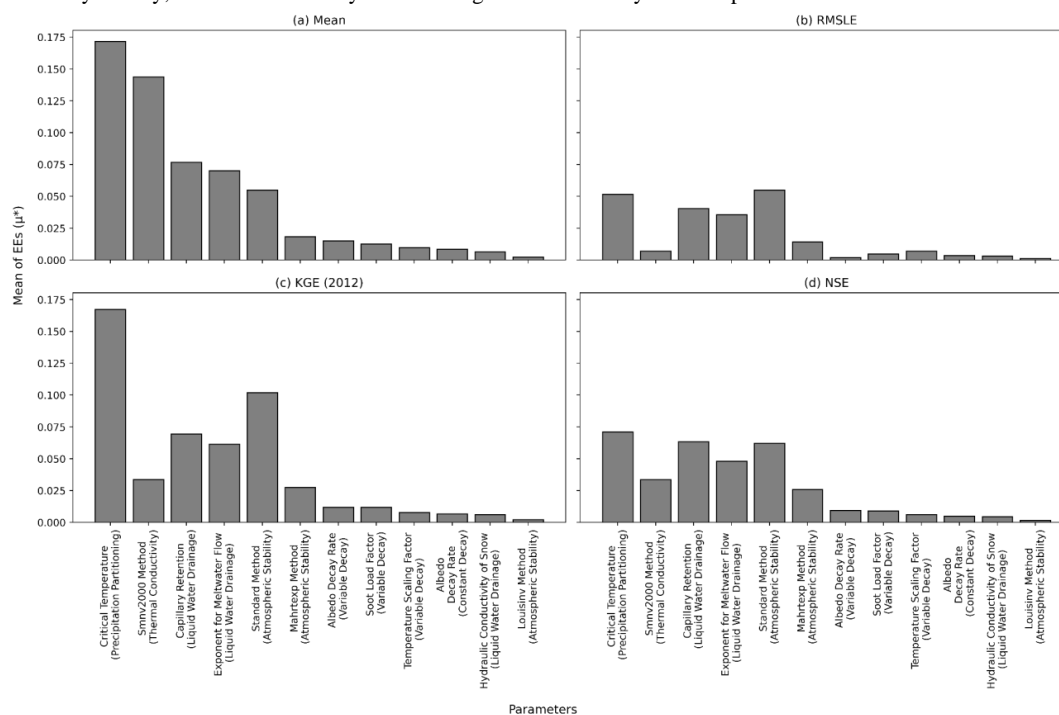
Figure 4: Qualitative sensitivity of parameters and parametrizations used in snow modelling process. Scatter plot of the Mean as the performance metric against parameter ranges.



279 **3.4 Quantitative sensitivity analysis**

280 To further examine the accuracy of these qualitative findings, a quantitative sensitivity analysis was employed as
 281 discussed in section 3.2.2. The Morris Method was used to estimate the Elementary Effects (EEs) for each of the
 282 model parameters. The variance in the ranking of parameters' accuracy prediction by different performance metrics
 283 prompted us to develop Elementary Effect functions using all the metrics and compare the sensitivity results. This
 284 was done to identify a system-scale performance metric that can consistently describe the observed sensitivities
 285 through scattered and perturbation plots.

286 A bar plot depicting the mean of Elementary Effects was developed accordingly and is shown in Figure 6. The plot
 287 shows a sensitivity analysis of all parameters and parametrizations using four different performance metrics. The
 288 parameters are sorted in descending sensitivity order, from the highest to the lowest, as determined by the mean snow
 289 depth. At a first glance, it can be seen that the performance metrics, which were predicting the accuracy of simulations
 290 relatively closely, exhibit substantially different degrees of sensitivity for each parameter.



291 **Figure 5:** Mean of Elementary Effects estimated using four performance metrics; (a) Mean, (b) RMSLE (c) KGE, and
 292 (d) NSE.
 293
 294

295 It can be observed that the critical temperature for rainfall, which determines the partitioning of incoming precipitation
 296 into rain and snow, is the most sensitive parameter in determining the depth of the snowpack. This prediction is
 297 consistent with previous observations made through perturbation plots in Figures 3 and 4, where a significant
 298 fluctuation in snow depth was observed by changing the critical temperature within its range. It was interesting to note
 299 that regardless of the performance metrics chosen, parameters such as the hydraulic conductivity of snow, and the
 300 constant and variable albedo decay rates, were consistently identified as the least sensitive in snow process modeling.
 301 This observation leads to the conclusion that different performance metrics can be effective in determining the

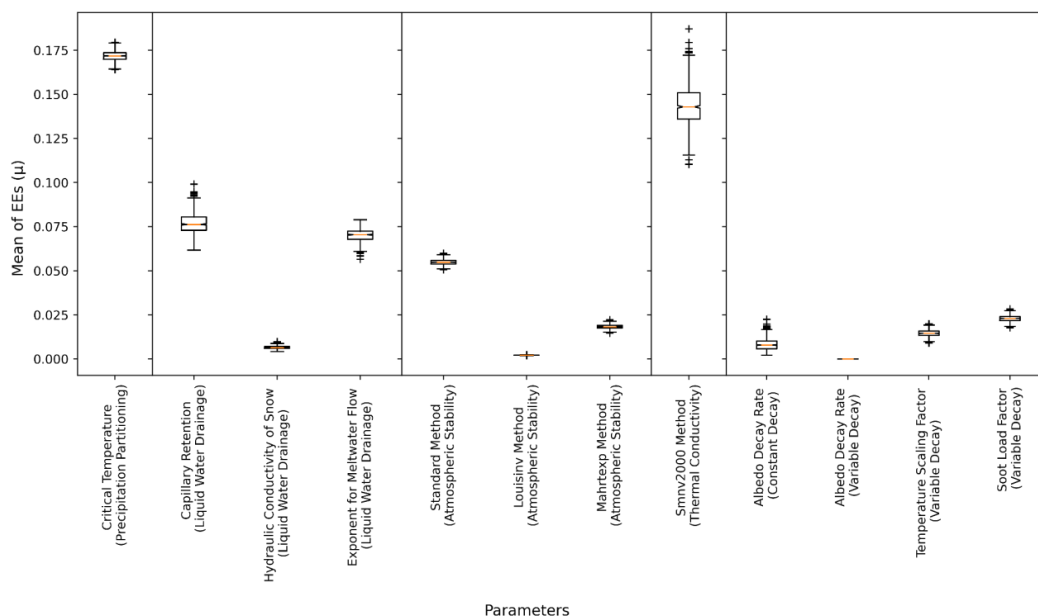


302 sensitivity indices of the least sensitive parameters. The discrepancy lies in quantifying the magnitude and rank of
 303 parameters with relatively higher sensitivities.

304 A very interesting result in Figure 5 is the difference in sensitivity for parameters in the thermal conductivity
 305 parameterization for the performance metrics that quantify differences in the mean (top left subplot in Figure 5) from
 306 the performance metrics that quantify differences in the simulated and observed time series (i.e., the RMSLE, KGE,
 307 and NSE, shown in the top-right, bottom-left, and bottom right subplots of Figure 5). These differences in model
 308 sensitivity can be explained through inspection of Figure 3, where the differences between the simulations with lowest
 309 thermal conductivity (blue line) have differences with the observations that are of opposing sign to the model
 310 simulations with the highest thermal conductivity (green line). Importantly, even though the snow depth time series
 311 are quite different, the performance metrics are quite similar. These results are a manifestation of equifinality, where
 312 different model trajectories can have similar performance. In this case, the impact of thermal conductivity parameters
 313 on the time series performance metrics are much smaller than would be expected from visual inspection of the impacts
 314 of thermal conductivity parameters on the snow depth time series.

315 To further quantify the rank and magnitude of the sensitivities, the means of Elementary Effects were bootstrapped to
 316 create a box and whisker plot, as shown in Figure 6. The parameters in the box and whisker plot are sorted to display
 317 the water balance fluxes (i.e., precipitation partitioning and liquid water flow) first, followed by the energy balance
 318 fluxes (i.e., atmospheric stability, thermal conductivity, and albedo).

319 Overall, it is noticeable that water balance fluxes exhibit higher sensitivity than energy balance in simulating snow
 320 processes.



321
 322

323 **Figure 6:** Mean of Elementary Effects developed using the Mean performance metric. The boxes show the
 324 interquartile range (25th, 50th, and 75th percentiles) and the whiskers represent the maximum and minimum limits of
 325 the mean of EEs.

326
 327
 328

Accordingly, the critical temperature of rain is the most sensitive parameter among the water balance parameters,
 while the thermal conductivity of snowpack is the most sensitive parameter among the energy balance parameters. As



329 expected, the albedo parameters, whether constant or variable, are among the least sensitive components in the snow
330 modelling processes. Figure 6 also shows that the parameters associated with the drainage of liquid from the
331 snowpack, namely capillary retention, and exponent of meltwater flow, have almost equally high sensitivities. In
332 contrast, the hydraulic conductivity of the snowpack seems to be among the least influential parameters in determining
333 the depth of snow. The insensitivity of the latter parameter is in alignment with the observations from perturbation
334 (Figure 4) and scattered plots (Figure 5).

335 The third panel of the boxplots in Figure 6 compares the sensitivity of three different atmospheric stability
336 parametrizations, showing that the critical Richardson number (Standard method) is the most sensitive among the
337 three methods. The reason for the high sensitivity of the Standard method may be attributed to the Richardson number
338 being in the numerator with an exponential power, as opposed to the other two methods, where the atmospheric
339 stability has an inverse relationship with the Richardson number. This sensitivity analysis denotes that water balance
340 parametrizations (i.e., critical temperature of rain) are much more sensitive than the energy balance (i.e., variable
341 albedo decay rate), as demonstrated by the comparison of the highest and lowest ends of flux spectrums.

342
343 The study's new insights suggest that water balance parameterizations are more sensitive than energy balance fluxes.
344 This finding highlights the importance of accurately representing the water balance processes in snow models, which
345 can improve the accuracy of snowmelt predictions. Additionally, the study suggests that modular and flexible
346 frameworks such as SUMMA enable identifying and isolating sensitive parameters, thereby improving the sensitivity
347 analysis of snow models.

348

349 **4 Conclusion**

350 This work presents the results of a sensitivity study of model simulations of snow processes in the Reynolds Mountain
351 East research catchment using a flexible, extensible, and modular hydrological framework. Through the analysis
352 conducted in this study, the following conclusions can be drawn:

353

- 354 • The use of a modular and flexible framework enables identifying and isolating parameters and parametrizations,
355 which in turn enables comprehensive sensitivity analysis.
- 356 • The sensitivity of performance metrics to perturbations in model parameters is contaminated by equifinality. We
357 illustrate some cases in this paper where parameter perturbations lead to similar performance metrics for quite
358 different snow depth time series. Given that many published parameter sensitivity studies are based on the
359 sensitivity of performance metrics to model parameters, the conclusions from many model sensitivity analysis
360 studies may not be trustworthy. It is hence crucial to select metrics for sensitivity analysis that accurately represent
361 the system-scale behavior. This would improve quantifying the magnitude and ranking of sensitivity indices.
- 362 • In the specific case of snow modeling in the Reynolds Mountain East research catchment, water balance fluxes are
363 generally more sensitive than energy balance fluxes. Among the parameters, the critical temperature of rain is the
364 most sensitive, while the albedo decay rate is the least sensitive.

365 There are several limitations of this study that can be explored in future research. This study used Elementary Effects
366 to conduct the sensitivity analysis. Although the Elementary Effect method is useful for models with a large number
367 of uncertainty factors, it does not quantify the relative importance of inputs. Additionally, the sensitivity analysis was
368 performed by isolating each snow modeling parameter and analyzing its effect on the system individually. This
369 approach limited the potential interactions between fluxes and may have affected the sensitivity rank and magnitude
370 of the parameters. Application of methods like variance-based sensitivity analysis methods can address these
371 limitations.



372

373 **Acknowledgement**

374 The authors acknowledge the cloud computational support from the Consortium of Universities for the Advancement
375 of Hydrologic Science, Incorporated (CUAHSI).

376

377 **Code and data availability**

378 The code and data used for this study can be obtained by directly contacting the corresponding author.

379

380 **Author contributions**

381 AK, MSA, TK, and YM designed the study and carried out the analysis. AK, MSA, TK, and YM wrote the manuscript,
382 with contributions and reviews from MPC and HL. All the authors contributed to the discussion and revision of the
383 manuscript.

384

385 **Competing interests**

386 The authors declare that they have no conflicts of interest.

387

388

389 **Appendix A**

390 4.1.1 Precipitation Partitioning

391 The parameterization to partition precipitation into rain and snow is a function of wet-bulb temperature (Clark et al.,
392 2015c; Marks et al., 2013), parametrized as a linear function that describes the temporal variability of the wetbulb
393 temperature over a model time step. The minimum and maximum wetbulb temperature over a model time step are
394 defined as

395

$$T_{max} = T_{wet} + T_{range}/2$$

396

$$T_{min} = T_{wet} - T_{range}/2$$

397 where T_{wet} is the wetbulb temperature and T_{range} defines the temporal variability of the wetbulb temperature over a
398 model time step. The fraction of precipitation that falls as rain, f_{rain} , is then defined based on a critical value of the
399 wetbulb temperature, T_{crit} , as

400

$$f_{rain} = \begin{cases} 0 & T_{max} < T_{crit} \\ \frac{T_{max} - T_{crit}}{T_{max} - T_{min}} & T_{min} \leq T_{crit} \leq T_{max} \\ 1 & T_{min} > T_{crit} \end{cases}$$

401

and the fraction of precipitation that falls as snow, $f_{snow} = 1 - f_{rain}$. The default value for T_{crit} is 0°C.

402 4.1.2 Liquid Water Flow

403 The storage and transmission of liquid water in the snowpack in SUMMA is parameterized as gravity drainage based
404 on the (Colbeck, 1976; Colbeck and Anderson, 1982) and calculated as follows:

405

$$q = k \left(\frac{\theta_{liq} - \theta_{res}}{\phi - \theta_{res}} \right)^c$$

406

407 where q is the drainage flux, k is the conductivity of snowpack [$m s^{-1}$], θ_{liq} is the current volumetric water content [-],
408 θ_{res} is the residual volumetric water content [-], ϕ is the available fraction of pore spaces [-], and c is non-linearity
409 coefficient [-]. As such, the liquid water flow in snow is controlled by k , θ_{res} , c .



410 4.1.3 Snow Albedo

411 Two semi-empirical options are implemented in SUMMA for the snow albedo parameterization:

412

413 • Variable Decay: This option is derived from Biosphere-Atmosphere Transfer Scheme (BATS) described by
414 Yang et al. (1997) where the albedo decay rate varies as snow properties change over time. BATS represents
415 the albedo separately for visible and near-infrared wavelengths as different wavelengths of solar radiation
416 are absorbed and reflected differently by the snowpack. The direct-beam albedo in BATS is set equal to the
417 diffuse albedo plus an additive factor at high solar zenith angles meaning that the diffuse albedo is the average
418 reflectivity of the snow surface over all angles of incidence, while the additive factor represents the additional
419 reflectivity of the snow surface at low solar zenith angles (Clark et al 2015a, 2015c; Yang et al., 1997). The
420 variable decay albedo parameterization is given as

421
$$\frac{d\alpha}{dt} = \kappa\alpha$$

422
$$\kappa = \kappa_0 (r_1 + r_2 + r_3)$$

423

424 where, α is the snow surface albedo, κ_0 is the time delay scaling factor, r_1 represents effects of grain growth due to
425 vapor diffusion, r_2 represents the additional effects of grain growth when the snow temperature is near the freezing
426 point, and r_3 is an adjustable parameter representing effects of dirt and soot.

427

428 • Constant Decay: This option is derived from the Canadian Land Surface Scheme (CLASS) described by
429 Verseghy (1991) where the albedo decay rate, which controls the rate at which the snow albedo adjusts to
430 changes in snow properties, is temporally constant. CLASS uses two decay curves, one for periods of
431 accumulation and the other for melting periods which is because the physical processes that affect snow
432 albedo, such as grain growth and meltwater formation, are different during these two periods. This approach
433 assumes that the direct beam and diffusive albedos are identical, as the difference between the two is only
434 distinct at high solar zenith angles when shortwave radiation fluxes are small (Clark et al., 2015a, 2015c;
435 Verseghy, 1991). The constant decay albedo parameterization is given simply as

436
$$\kappa = \kappa_0$$

437 4.1.4 Atmospheric Stability

438 A considerable amount of the energy involved in snowmelt or ice ablation is transferred from the atmosphere through
439 turbulent fluxes (see Figure 2). The turbulent transfer process in the surface boundary layer generates sensible and
440 latent heat fluxes, which are recognized as important contributors to the energy input for melting snow cover (Morris,
441 1989). These fluxes can be expressed as the covariance of fluctuations in vertical velocity. While it is feasible to
442 directly measure these covariances and obtain accurate estimates of the fluxes, such measurements are seldom
443 accessible. In numerous experimental and modeling studies, it becomes essential to represent these fluxes through
444 parameterization. Three options are implemented in SUMMA for the atmospheric stability parametrization based on
445 the bulk Richardson number:

446

447 • Critical Richardson Number (Standard): This option is the default atmospheric stability option in SUMMA
448 and derived from Anderson (1976) which calculates atmospheric stability based on the vertical gradient of
449 potential temperature and the horizontal wind speeds. The bulk Richardson number (Ri) is defined as the
450 ratio of the potential energy available for turbulence to the kinetic energy associated with the vertical shear
451 of the horizontal wind. This method assumes that the eddy diffusivity for heat is constant and depends only
452 on the bulk Richardson number. Implementing this method in SUMMA is based on the use of atmospheric
453 stability classes, which are assigned based on the value of the bulk Richardson number (Anderson, 1976;
454 Clark et al. 2015a, 2015c;). The atmospheric stability correction (F) for the stable condition can be calculated



455 by using the following formula:

456

457

$$F = \begin{cases} (1 - 5R_i)^2 & R_i < R_{ic} \\ 0 & R_i \geq R_{ic} \end{cases}$$

458

459

where, R_i is the bulk Richardson Number [-].

460

461

462

- Louis79 “b” parameter (Louisinv): This option is derived from Louis (1979), who parameterizes the atmospheric stability correction (F) for stable conditions as:

463

$$F = \frac{1}{(1 + b'R_i)^2}$$

464

where, b' = Louis (1979) “b” parameter / 2 [-].

465

466

467

- Mahrt87 eScale (MahrtExp): This option is derived from Mahrt (1987), who considers spatial averaging of subgrid processes. where the atmospheric stability correction (F) for stable conditions is given as:

468

$$F = e^{-mR_i}$$

469

where, m = Mahrt exp coefficient [-].

470

471 4.1.5 Thermal Conductivity

472

Four empirical options are implemented in SUMMA to parameterize the thermal conductivity of snow:

473

474

Yen 1965: This option is derived from Yen (1965) who conducted experiments to measure the effective thermal conductivity (K) of naturally compacted snow at different densities. The results of Yen's experiments showed that the effective thermal conductivity of ventilated snow strongly depends on the square of its density plus the effect of dry airflow. Yen concluded that turbulence introduced by the air stream reduces the resistance for the simultaneous transfer processes of heat and mass (i.e., water vapor diffusion) and increases the thermal conductivity of snow. Accordingly, as the density of snow and mass flow rate of dry air increases, the effective thermal conductivity also increases. In the absence of airflow, Yen's equation reduces to a relationship between the effective thermal conductivity and the snow density.

482

483

$$K = 3.217 \times 10^{-6} \gamma_s^2$$

484

485

where, γ_s is the bulk density of snow [$kg.m^{-3}$].

486

487

488

489

490

491

492

493

494

495

- melr 1977: This option is derived from Mellor (1977) who described heat transfer in a dry snowpack as a process involving conduction (e.g., in the network of ice grains and bonds, and airspaces and pores), convection and radiation (e.g., across pores which were assumed negligible), and water vapor diffusion through voids; however, considering empirical curves of the snow thermal conductivity developed by a number of researchers, he concluded that engineering applications the thermal conductivity of the dense snow and bubbly ice can be assumed to be proportional to the square of the snow density (discounting finer details or complications). Accordingly, SUMMA adopted a fit to the quadratic snow density versus thermal conductivity data provided by Mellor (Mellor 1977; Clark et al. 2015a, 2015c).

496

$$K = 2.576 \times 10^{-6} \gamma_s^2 + 7.4 \times 10^2$$

497

498

499

- jrdn 1991: This option is derived from Jordan (1991) who proposed to estimate the effective thermal conductivity of snow by accounting for ice and air conduction and vapour diffusion through the voids.



500 Accordingly, Jordan's parametrization includes a thermal conductivity term with a polynomial relationship
501 to the snow density together with constant values for the conductivity of air and ice in the snowpack.
502 Adjustable parameters in Jordan's equation have been selected so that the effective thermal conductivity fits
503 the data of Yen (1962) and extrapolates to ice conductivity when the snow density is that of ice.

$$504 \quad K = K_a + (7.75 \times 10^{-5} \gamma_s + 1.105 \times 10^{-6} \gamma_s^2)(K_i - K_a)$$

505
506
507 where, K_a is thermal conductivity of air = $0.023 [W K^{-1} m^{-1}]$ and K_i is thermal conductivity of ice = $2.29 [W K^{-1} m^{-1}]$.

- 508
- 509 • smnv 2000: This option is derived from Smirnova et al. (2000) where a constant value for the thermal
510 conductivity of snow (set equal to $0.35 W K^{-1} m^{-1}$) was considered which lies within the range of this variable
511 for old and new snow as per a study.

512
513
514



515 5. References

- 516 Anderson, E. A.: A Point Energy and Mass Balance Model of a Snow Cover, NOAA Tech. Rep. NWS 19,
517 Maryland, USA, 150 pp., 1976.
- 518 Best, M. J., Pryor, M., Clark, D. B., Rooney, G. G., Essery, R. L. H., Ménard, C. B., Edwards, J. M., Hendry, M. A.,
519 Porson, A., Gedney, N., Mercado, L. M., Sitch, S., Blyth, E., Boucher, O., Cox, P. M., Grimmond, C. S. B., and
520 Harding, R. J.: The Joint UK Land Environment Simulator (JULES), model description – Part 1: Energy and water
521 fluxes, *Geosci. Model Dev.*, 4, 677–699, <https://doi.org/10.5194/gmd-4-677-2011>, 2011.
- 522 Campolongo, F., Cariboni, J., and Saltelli, A.: An effective screening design for sensitivity analysis of large models,
523 *Environ. Model. Softw.*, 22, 1509–1518, <https://doi.org/10.1016/j.envsoft.2006.10.004>, 2007.
- 524 Chamberlin, T. C.: The Method of Multiple Working Hypotheses, *Science (80-.)*, ns-15, 92–96,
525 <https://doi.org/10.1126/science.ns-15.366.92>, 1890.
- 526 Clark, M. P., Kavetski, D., and Fenicia, F.: Pursuing the method of multiple working hypotheses for hydrological
527 modeling, *Water Resour. Res.*, 47, <https://doi.org/10.1029/2010WR009827>, 2011.
- 528 Clark, M. P., Nijssen, B., Lundquist, J. D., Kavetski, D., Rupp, D. E., Woods, R. A., Freer, J. E., Gutmann, E. D.,
529 Wood, A. W., Brekke, L. D., Arnold, J. R., Gochis, D. J., and Rasmussen, R. M.: A unified approach for process-
530 based hydrologic modeling: 1. Modeling concept, *Water Resour. Res.*, 51, 2498–2514,
531 <https://doi.org/10.1002/2015WR017198>, 2015a.
- 532 Clark, M. P., Nijssen, B., Lundquist, J. D., Kavetski, D., Rupp, D. E., Woods, R. A., Freer, J. E., Gutmann, E. D.,
533 Wood, A. W., Gochis, D. J., Rasmussen, R. M., Tarboton, D. G., Mahat, V., Flerchinger, G. N., and Marks, D. G.: A
534 unified approach for process-based hydrologic modeling: 2. Model implementation and case studies, *Water Resour.*
535 *Res.*, 51, 2515–2542, <https://doi.org/10.1002/2015WR017200>, 2015b.
- 536 Clark, M. P., Nijssen, B., Lundquist, J. D., Kavetski, D., Rupp, D. E., Woods, R. A., Freer, J. E., Gutmann, E. D.,
537 Wood, A. W., Brekke, L. D., Arnold, J. R., Gochis, D. J., Rasmussen, R. M., Tarboton, D. G., Mahat, V.,
538 Flerchinger, G. N., and Marks, D. G.: The structure for unifying multiple modeling alternatives (SUMMA), Version
539 1.0: Technical Description, Boulder, Colorado, 2015c.
- 540 Colbeck, S. C.: An analysis of water flow in dry snow, *Water Resour. Res.*, 12, 523–527,
541 <https://doi.org/10.1029/WR012i003p00523>, 1976.
- 542 Colbeck, S. C. and Anderson, E. A.: The permeability of a melting snow cover, *Water Resour. Res.*, 18, 904–908,
543 <https://doi.org/10.1029/WR018i004p00904>, 1982.
- 544 Flerchinger, G. N., Reba, M. L., and Marks, D.: Measurement of Surface Energy Fluxes from Two Rangeland Sites
545 and Comparison with a Multilayer Canopy Model, *J. Hydrometeorol.*, 13, 1038–1051, [https://doi.org/10.1175/JHM-](https://doi.org/10.1175/JHM-D-11-093.1)
546 [D-11-093.1](https://doi.org/10.1175/JHM-D-11-093.1), 2012.
- 547 Gupta, H. V., Clark, M. P., Vrugt, J. A., Abramowitz, G., and Ye, M.: Towards a comprehensive assessment of
548 model structural adequacy, <https://doi.org/10.1029/2011WR011044>, 2012.
- 549 Gupta, H. V., Kling, H., Yilmaz, K. K., and Martinez, G. F.: Decomposition of the mean squared error and NSE
550 performance criteria: Implications for improving hydrological modelling, *J. Hydrol.*, 377, 80–91,
551 <https://doi.org/10.1016/j.jhydrol.2009.08.003>, 2009.
- 552 Hanson, C. L., Marks, D., and Van Vactor, S. S.: Long-term climate database, Reynolds Creek Experimental
553 Watershed, Idaho, United States, *Water Resour. Res.*, 37, 2839–2841, <https://doi.org/10.1029/2001WR000417>,
554 2001.
- 555 Jordan, R.: A One-Dimensional Temperature Model for a Snow Cover, 1991.
- 556 Kling, H., Fuchs, M., and Paulin, M.: Runoff conditions in the upper Danube basin under an ensemble of climate
557 change scenarios, *J. Hydrol.*, 424–425, 264–277, <https://doi.org/10.1016/j.jhydrol.2012.01.011>, 2012.
- 558 Knoben, W. J. M., Freer, J. E., and Woods, R. A.: Technical note: Inherent benchmark or not? Comparing Nash--
559 Sutcliffe and Kling--Gupta efficiency scores, *Hydrol. Earth Syst. Sci.*, 23, 4323–4331, [https://doi.org/10.5194/hess-](https://doi.org/10.5194/hess-23-4323-2019)
560 [23-4323-2019](https://doi.org/10.5194/hess-23-4323-2019), 2019.
- 561 Koster, R. D. and Milly, P. C. D.: The Interplay between Transpiration and Runoff Formulations in Land Surface
562 Schemes Used with Atmospheric Models, *J. Clim.*, 10, 1578–1591, [https://doi.org/10.1175/1520-](https://doi.org/10.1175/1520-0442(1997)010<1578:TIBTAR>2.0.CO;2)
563 [0442\(1997\)010<1578:TIBTAR>2.0.CO;2](https://doi.org/10.1175/1520-0442(1997)010<1578:TIBTAR>2.0.CO;2), 1997.
- 564 Lawrence, P. J. and Chase, T. N.: Representing a new MODIS consistent land surface in the Community Land
565 Model (CLM 3.0), *J. Geophys. Res. Biogeosciences*, 112, <https://doi.org/10.1029/2006JG000168>, 2007.
- 566 Louis, J.-F.: A Parametric Model of Vertical Eddy Fluxes in the Atmosphere, *Bound. Layer Meteorol.*, 17, 187–202,
567 1979.
- 568 Mahrt, L.: Grid-Averaged Surface Fluxes, *Mon. Weather Rev.*, 115, 1550–1560, 1987.
- 569 Marks, D., Winstral, A., Reba, M., Pomeroy, J., and Kumar, M.: An evaluation of methods for determining during-



- 570 storm precipitation phase and the rain/snow transition elevation at the surface in a mountain basin, *Adv. Water*
571 *Resour.*, 55, 98–110, <https://doi.org/https://doi.org/10.1016/j.advwatres.2012.11.012>, 2013.
- 572 Mellor, M.: Engineering Properties of Snow, *J. Glaciol.*, 19, 15–66, <https://doi.org/10.3189/s002214300002921x>,
573 1977.
- 574 Morris, E. M.: Turbulent transfer over snow and ice, *J. Hydrol.*, 105, 205–223, <https://doi.org/10.1016/0022->
575 1694(89)90105-4, 1989.
- 576 Nash, J. E. and Sutcliffe, J. V.: River flow forecasting through conceptual models part I — A discussion of
577 principles, *J. Hydrol.*, 10, 282–290, [https://doi.org/10.1016/0022-1694\(70\)90255-6](https://doi.org/10.1016/0022-1694(70)90255-6), 1970.
- 578 Niu, G.-Y., Yang, Z.-L., Mitchell, K. E., Chen, F., Ek, M. B., Barlage, M., Kumar, A., Manning, K., Niyogi, D.,
579 Rosero, E., Tewari, M., and Xia, Y.: The community Noah land surface model with multiparameterization options
580 (Noah-MP): 1. Model description and evaluation with local-scale measurements, *J. Geophys. Res. Atmos.*, 116,
581 <https://doi.org/10.1029/2010JD015139>, 2011.
- 582 Noacco, V., Sarrazin, F., Pianosi, F., and Wagener, T.: Matlab/R workflows to assess critical choices in Global
583 Sensitivity Analysis using the SAFE toolbox, *MethodsX*, 6, 2258–2280, <https://doi.org/10.1016/j.mex.2019.09.033>,
584 2019.
- 585 Pianosi, F., Sarrazin, F., and Wagener, T.: A Matlab toolbox for Global Sensitivity Analysis, *Environ. Model.*
586 *Softw.*, 70, 80–85, <https://doi.org/10.1016/j.envsoft.2015.04.009>, 2015.
- 587 Reba, M. L., Link, T. E., Marks, D., and Pomeroy, J.: An assessment of corrections for eddy covariance measured
588 turbulent fluxes over snow in mountain environments, *Water Resour. Res.*, 45,
589 <https://doi.org/10.1029/2008WR007045>, 2009.
- 590 Reba, M. L., Marks, D., Seyfried, M., Winstral, A., Kumar, M., and Flerchinger, G.: A long-term data set for
591 hydrologic modeling in a snow-dominated mountain catchment, *Water Resour. Res.*, 47,
592 <https://doi.org/10.1029/2010WR010030>, 2011.
- 593 Reba, M. L., Pomeroy, J., Marks, D., and Link, T. E.: Estimating surface sublimation losses from snowpacks in a
594 mountain catchment using eddy covariance and turbulent transfer calculations, *Hydrol. Process.*, 26, 3699–3711,
595 <https://doi.org/10.1002/hyp.8372>, 2012.
- 596 Reba, M. L., Marks, D., Link, T. E., Pomeroy, J., and Winstral, A.: Sensitivity of model parameterizations for
597 simulated latent heat flux at the snow surface for complex mountain sites, *Hydrol. Process.*, 28, 868–881,
598 <https://doi.org/10.1002/hyp.9619>, 2014.
- 599 Roberts, W., Williams, G. P., Jackson, E., Nelson, E. J., and Ames, D. P.: Hydrostats: A Python Package for
600 Characterizing Errors between Observed and Predicted Time Series, *Hydrology*, 5,
601 <https://doi.org/10.3390/hydrology5040066>, 2018.
- 602 Robins, J. S., Kelly, L. L., and Hamon, W. R.: Reynolds Creek in southwest Idaho: An outdoor hydrologic
603 laboratory, *Water Resour. Res.*, 1, 407–413, <https://doi.org/10.1029/WR001i003p00407>, 1965.
- 604 Saltelli, A., Ratto, M., Andres, T., Campolongo, F., Cariboni, J., Gatelli, D., Saisana, M., and Tarantola, S.: Global
605 sensitivity analysis: the primer, John Wiley & Sons, 2008.
- 606 Seyfried, M. S., Grant, L. E., Marks, D., Winstral, A., and McNamara, J.: Simulated soil water storage effects on
607 streamflow generation in a mountainous snowmelt environment, Idaho, USA, *Hydrol. Process.*, 23, 858–873,
608 <https://doi.org/10.1002/hyp.7211>, 2009.
- 609 Smimova, T. G., Brown, J. M., Benjamin, S. G., and Kim, D.: Parameterization of cold-season processes in the
610 MAPS land-surface scheme, *J. Geophys. Res. Atmos.*, 105, 4077–4086, <https://doi.org/10.1029/1999JD901047>,
611 2000.
- 612 Sridhar, V. and Nayak, A.: Implications of climate-driven variability and trends for the hydrologic assessment of the
613 Reynolds Creek Experimental Watershed, Idaho, *J. Hydrol.*, 385, 183–202,
614 <https://doi.org/10.1016/j.jhydrol.2010.02.020>, 2010.
- 615 Tarboton, D. G., Ames, D. P., Horsburgh, J. S., Goodall, J. L., Couch, A., Hooper, R., Bales, J., Wang, S.,
616 Castronova, A., Seul, M., Idaszak, R., Li, Z., Dash, P., Black, S., Ramirez, M., Yi, H., Calloway, C., and Cogswell,
617 C.: HydroShare retrospective: Science and technology advances of a comprehensive data and model publication
618 environment for the water science domain, *Environ. Model. Softw.*, 172, 105902,
619 <https://doi.org/10.1016/j.envsoft.2023.105902>, 2024.
- 620 Verseghy, D. L.: Class—A Canadian land surface scheme for GCMS. I. Soil model, *Int. J. Climatol.*, 11, 111–133,
621 <https://doi.org/10.1002/joc.3370110202>, 1991.
- 622 Willmott, C. J. and Matsuura, K.: Advantages of the mean absolute error (MAE) over the root mean square error
623 (RMSE) in assessing average model performance, *Clim. Res.*, 30, 79–82, 2005.
- 624 Winstral, A. and Marks, D.: Long-term snow distribution observations in a mountain catchment: Assessing



625 variability, time stability, and the representativeness of an index site, *Water Resour. Res.*, 50, 293–305,
626 <https://doi.org/10.1002/2012WR013038>, 2014.
627 Yang, Z., Dickinson, R. E., Robock, A., and Vinnikov, K. Y.: Validation of the Snow Submodel of the Biosphere-
628 Atmosphere Transfer Scheme with Russian Snow Cover and Meteorological Observational Data, 1997.
629 Yen, Y.-C.: Effective thermal conductivity and water vapor diffusivity of naturally compacted snow, *J. Geophys.*
630 *Res.*, 70, 1821–1825, <https://doi.org/10.1029/jz070i008p01821>, 1965.
631